

Characterization and Modeling of Wireless Channels for Networked Robotic and Control Systems – A Comprehensive Overview

Yasamin Mostofi, Alejandro Gonzalez-Ruiz, Alireza Gaffarkhah and Ding Li
Cooperative Network Lab, Department of Electrical and Computer Engineering
University of New Mexico, Albuquerque, NM 87113, USA
Email: {ymostofi,agon,alinem,liding}@ece.unm.edu

Abstract—The goal of this paper is to serve as a reference for researchers in robotics and control that are interested in realistic modeling, theoretical analysis and simulation of wireless links. To realize the full potentials of networked robotic systems, an integration of communication issues with motion planning/control is necessary. While considerable progress has been made in the area of networked robotic systems, communication channels are typically considered ideal or ideal within a certain radius of the transmitter, both considerable oversimplifications of wireless channels. It is the goal of this paper to provide a comprehensive overview of the key characteristics of wireless channels, as relevant to networked robotic operations. In particular, we provide a probabilistic framework for characterization of the underlying multi-scale dynamics of a wireless link: *small-scale fading, large-scale fading and path loss*. We furthermore confirm these mathematical models with channel measurements made in our building. We also discuss channel characterization based on the knowledge available on the geometry and dielectric properties of the environment.

I. MOTIVATION

The unprecedented growth of sensing, communication and computation in the past few years has the potential of fundamentally changing the way we understand and process information. The sensor network revolution has created the possibility of exploring and controlling the environment in ways not possible before. The vision of a multi-agent robotic network cooperatively learning and adapting in harsh unknown environments to achieve a common goal is closer than ever. In order to realize this vision, however, an integrative approach to communication and control issues is essential.

In the robotics and control community, considerable progress has been made in the area of networked robotic and control systems. Similarly, in the communications systems community, rich literature was developed, over the past decades, for the characterization and modeling of wireless channels. However, the knowledge available on wireless link characterization has rarely been used in networked robotic/control literature, i.e. ideal or over-simplified models have mainly been used so far. It is therefore the goal of this paper to provide a reference for the characterization and modeling of wireless channels for networked robotic operations.

In a realistic communication setting, such as an urban area or indoor environment, Line-Of-Sight (LOS) communication may not be possible due to the existence of several objects

that can attenuate, reflect, diffract or block the transmitted signal. The received signal power typically experiences considerable variations and can change drastically in even a small distance. As an example, consider Fig. 1, where channel measurements in the Electrical and Computer Engineering (ECE) building at UNM are shown. It can be seen that channel can change drastically with a small movement of the robot. Communication between robotic units can be degraded due to factors such as shadowing, fading or distance-dependent path loss [1]. While these factors can degrade the overall performance of the robotic network considerably, multi-agent robotic and navigation literature typically consider ideal links or links that are ideal within a certain radius of the node.

In this paper, we provide a framework for understanding, abstraction, modeling and simulation of wireless channels for networked robotic and control applications, by tapping into the relevant knowledge available in wireless communication literature. Our experimental results furthermore assert these mathematical models. We start by probabilistic characterization of wireless channels and their underlying dynamics in Section II. Our mathematical framework is based on well-known references in wireless communication literature such as [1]–[3]. We then discuss different ways of characterizing a wireless channel based on the knowledge available on the environment in Section III. We conclude in Section IV.

II. A MULTI-SCALE CHARACTERIZATION OF WIRELESS CHANNELS

Wireless channels can be categorized into two main groups of narrowband and wideband [3], depending on the length of channel delay spread as compared to the transmission data rate. For narrowband channels, channel frequency response can be considered flat in the transmission bandwidth. This, however, is not the case for wideband channels. For most current robotic applications, the transmission rates are low enough to consider the channel to be narrowband. Therefore, in this paper we focus on narrowband channels. The framework of this paper can be easily extended to wideband channels by considering channel delay spread. Readers are referred to Chapter 3 of [3] for more details.

In general, exact mathematical characterization of a wireless channel is extremely challenging due to its time-varying and unpredictable nature. Blocking, reflection, scattering and

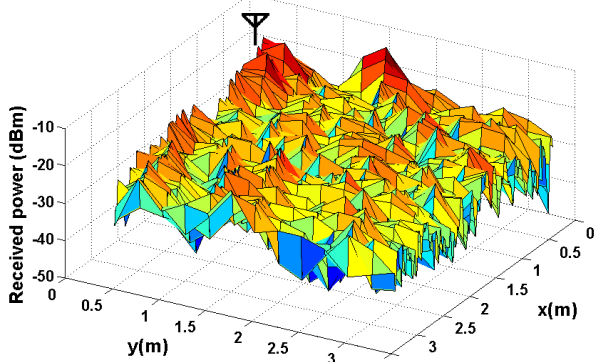
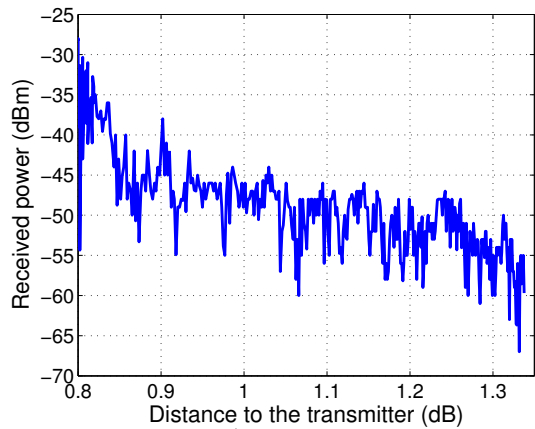


Fig. 1. Channel measurement (top) along a hallway in the basement of ECE building and (bottom) in the Cooperative Network Lab at the University of New Mexico.

diffraction are a few examples of phenomena that a transmitted wave experiences. One can possibly solve Maxwell's equations with proper boundary conditions that reflect all physical constraints of the environment. However, such calculation is difficult and requires the knowledge of several geometric and dielectric properties of the environment, which is not easily available. In wireless communication systems, it is therefore common to model the channel probabilistically with the goal of capturing its underlying dynamics. The utilized probabilistic models are the results of analyzing several empirical data over the years. In general, a communication channel between two robotic platforms can be modeled as a multi-scale dynamical system with three major dynamics: *small-scale fading*, *large-scale fading* and *path loss*. We first show an example of these three dynamics through an experiment. Fig. 2 shows the blueprint of a portion of the basement of the Electrical and Computer Engineering building at UNM. We used a Pioneer-AT robot to make several measurements along more than 70 routes in the basement, in order to map the received signal strength (each route is a straight line). The robot is equipped with an 802.11g wireless card with transmission at 2.4 GHz. The figure also shows a colormap of our measured received signal power for the transmitter at location#1. In this paper, we use this data for analysis and mathematical characterization.

Fig. 3 shows the received signal power across route 1, as marked in Fig. 2, for the transmitter at location#1 and

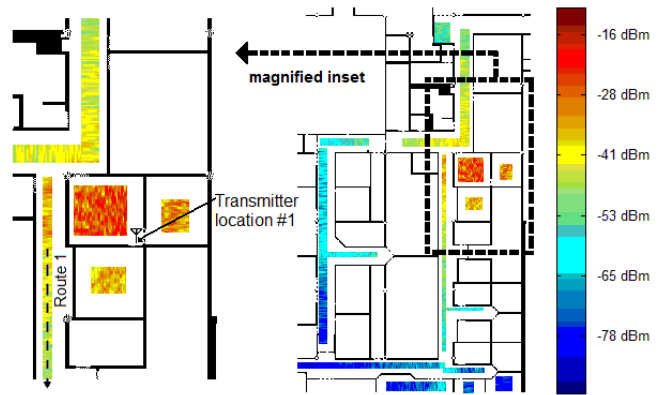


Fig. 2. (right) Blueprint of the portion of the basement of the ECE bldg. at UNM where channel measurements are collected – a colormap of the measured received signal power is superimposed on the map for the transmitter at location#1. (left) A magnified inset of the blueprint.

as a function of the distance to the transmitter. The three main dynamics of the received signal power are marked on the figure. As can be seen, the received power can have rapid spatial variations that are referred to as small-scale fading. By spatially averaging the received signal locally and over distances that channel can still be considered stationary, a slower dynamic emerges, which is called large-scale fading. Finally, by averaging over the variations of the large-scale fading, a distance-dependent trend is seen, which is referred to as path loss. In the next sections, we provide an understanding and modeling of these underlying dynamics.

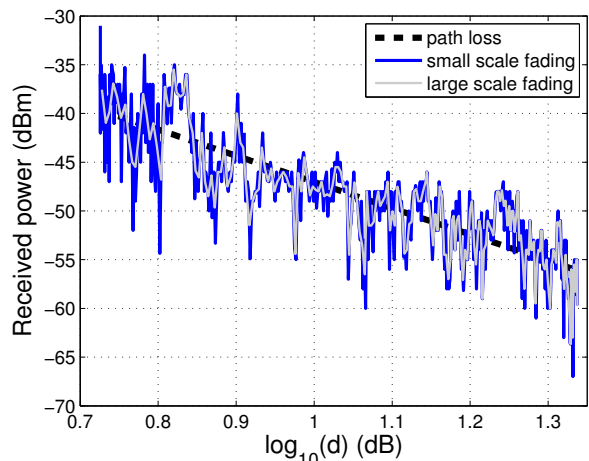


Fig. 3. Underlying dynamics of the received signal Power across route 1 of Fig. 2 and for transmitter location#1. The solid blue curve is the measured received power which exhibits small-scale fading. By averaging locally over small-scale variations, the underlying large-scale variations can be seen (light gray curve). The average of the large-scale variations then follows the distance-dependent path loss curve (dashed line).

A. Small-Scale Fading (Multipath Fading)

Due to the range of the carrier frequencies used for wireless transmissions, a wireless transmitted signal is considered a bandpass signal (See Appendix A of [3]). For the ease of mathematical derivations, however, it is common to work

with the baseband equivalent of the signal.¹ When a wireless transmission occurs, replicas of the transmitted signal will arrive at the receiver due to phenomena such as reflection and scattering. Each of these replicas is referred to as a path. Let $u(t)$ and $s(t)$ represent the baseband equivalent transmitted and received signals respectively. We have the following for the case of a mobile transmitter or receiver, by considering all the paths that arrive to the receiver:

$$s(t) = \underbrace{\sum_{n=1}^{N(t)} \alpha_n(t) u(t - \tau_n(t)) e^{j\phi_n(t) - j2\pi f_c \tau_n(t)}}_{r(t)} + w(t), \quad (1)$$

where $N(t)$ represents the total number of paths that arrive at the receiver at time t , f_c is the carrier frequency, and α_n , τ_n and ϕ_n are the attenuation, delay and Doppler phase shift of the n^{th} path respectively. $w(t)$ denotes sample of the receiver thermal noise at time t and $r(t)$ represents the noiseless part of the received signal. If both transmitter and receiver are moving, the phase term can be easily extended to account for double mobility [4]. Let $\tau_{\max}(t) = \max_n \tau_n(t)$ and $\tau_{\min}(t) = \min_n \tau_n(t)$. For narrowband channels, we have $u(t - \tau_{\max}(t)) \approx u(t - \tau_{\min}(t))$, resulting in $r(t) = u(t - \tau_{\min}(t))h(t)$, where

$$h(t) = \sum_{n=1}^{N(t)} \alpha_n(t) e^{j\phi_n(t) - j2\pi f_c \tau_n(t)} \quad (2)$$

represents the baseband equivalent channel. As can be seen, different paths can be added constructively or destructively depending on the phase terms of individual paths. As a result, with a small movement, the phase terms can change drastically, resulting in the rapid variations of the channel. Such rapid variations are referred to as small-scale fading (multipath fading) and can be seen from Fig. 3. The higher the number of reflectors and scatterers in the environment, the more severe small-scale variations could be.

1) *Parameters of Importance:* Let P_T represent the power of the transmitted signal. Then, $P_r(t) = \mathbb{E}[|r(t)|^2 | h(t)] = P_T |h(t)|^2$ represents the power of the noiseless part of the received signal. Received Signal to Noise Ratio, $\text{SNR}(t)$, an important parameter in characterizing the quality of a wireless link, is defined as the ratio of the received signal power divided by the receiver thermal noise power: $\text{SNR}(t) = \frac{P_r(t)}{P_w}$, where P_w is the power of $w(t)$. Received signal power and SNR are key factors in determining whether a received packet will be kept and used in the receiving robot or not. Since both are functions of $|h(t)|$ (P_T and P_w are time-invariant), we next focus on characterizing the underlying dynamics of $|h(t)|$.

2) *Distribution of Small-Scale Fading:* In the wireless communications literature, several efforts have been made in order to mathematically characterize the behavior of small-scale fading. As can be seen from Fig. 3, the small-scale

¹Let ξ_{bb} represent the baseband equivalent of the bandpass signal ξ . We have $\xi = \text{Re}\{\xi_{\text{bb}} e^{j2\pi f_c t}\}$, where f_c is the carrier frequency. Everything derived for the baseband equivalent can be equivalently extended to the original bandpass signal.

fading curve is non-stationary over large distances as its average is changing. Therefore, it is common to characterize the behavior of it over small enough distances where channel (or equivalently P_r and SNR) can be considered stationary. Then, the behavior of the average of the small-scale variations is characterized in order to address the behavior over larger distances, as we shall see in the next part. Over small enough distances where channel (or equivalently the receiver signal power) can be considered stationary, it can be mathematically shown that Rayleigh distribution is a good match for the distribution of $|h(t)|$ if there is no Line Of Sight (LOS) path while Rician provides a better match if an LOS exists. These distributions also match several empirical data. A more general distribution that was shown to match empirical data is Nakagami distribution [3], which has the following pdf for $z(t)$ where $z(t) = |h(t)|$:

$$p(z) = \frac{2m^m z^{2m-1}}{\Gamma(m) \overline{P}_z^m} \exp\left[\frac{-mz^2}{\overline{P}_z}\right], \quad (3)$$

for $m \geq 0.5$, where m is the fading parameter, $\overline{P}_z = \mathbb{E}[|h(t)|^2]$ and $\Gamma(\cdot)$ is the Gamma function. If $m = 1$, this distribution becomes Rayleigh whereas for $m = \frac{(m'+1)^2}{2m'+1}$, it is reduced to a Rician distribution with parameter m' . Similarly, distributions of the power of the channel ($|h|^2$), P_r and SNR can be derived by a change of variables. Such distributions can be very helpful in generating realistic communication links for the purpose of mathematical analysis as well as simulation in robotic networks.

3) *Justification of the Distribution for Small-Scale Fading:* While the aforementioned distributions matched several empirical data, as reported in wireless communications literature, mathematical justifications also exist. For instance, from Eq. 2, it can be seen that both the in-phase and quadrature components of $h(t)$ consist of a number of terms (as long as there are enough reflectors or scatterers). For the case of no LOS path, it can be shown that the in-phase and quadrature components are zero mean. Therefore, by evoking Central Limit Theorem, the in-phase and quadrature components will have a zero-mean normal distribution, resulting in a Rayleigh distribution for $|h(t)|$ and an exponential distribution for P_r and SNR.

Fig. 4 shows the probability density function (pdf) and cumulative distribution function (cdf) of a part of the small-scale variations² of the data of Fig. 3. It can be seen that the distribution of the gathered data matches power distribution for Nakagami fading with parameter $m = 1.9$ well. Note that since the distribution of the power of the received signal, P_r , is plotted, the figure does not show a Nakagami distribution directly. It shows the power distribution of Nakagami fading, i.e. the distribution of a non-negative variable whose square root has a Nakagami distribution.

B. Large-Scale Fading (Shadowing)

As discussed in the previous part, the received wireless signal is non-stationary over large distances. While small-

²The part is chosen such that the data can be considered stationary.

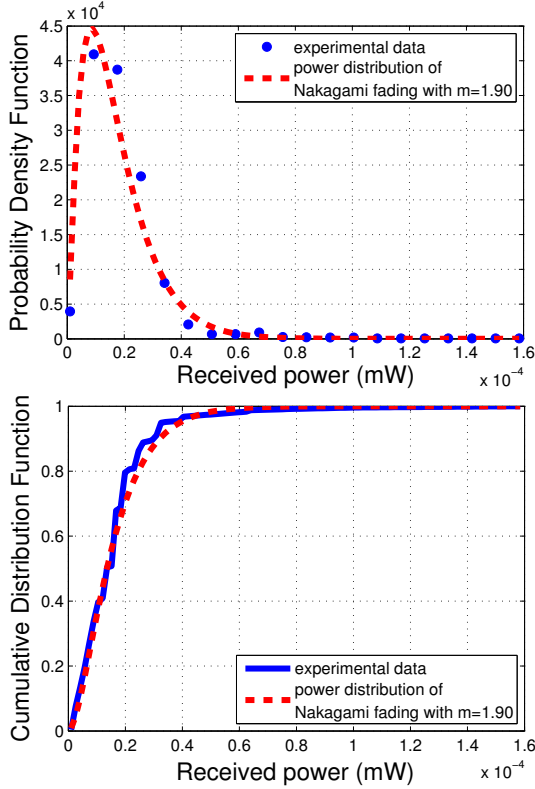


Fig. 4. Nakagami match for small-scale fading for gathered data in route 1 of Fig. 3 with transmitter at location#1 – (top) pdf and (bottom) cdf.

scale fading characterizes the behavior of the channel over a small distance, it does not suffice for characterizing the channel over larger distances. Small-scale variations are the result of a number of paths arriving at the receiver at approximately the same time but being added constructively or destructively depending on their phase terms, resulting in rapid variations. Once we average over small-scale variations, another dynamic can be observed which changes at a slower rate. Let $\bar{P}_z = \mathbb{E}[|h(t)|^2]$ represent average power of the channel (averaged over small-scale fading), as defined for Eq. 3. This signal (and similarly $\bar{P}_r = \bar{P}_z P_T$) varies over larger distances and is referred to as large-scale fading or shadowing. Large-scale fading is the result of the transmitted signal being possibly blocked by a number of obstacles before reaching the receiver. Empirical data has shown \bar{P}_z to have a lognormal distribution. Let $\bar{P}_{z,\text{dB}} = 10 \log_{10}(\bar{P}_z)$. We have the following for the distribution of $\bar{P}_{z,\text{dB}}$:

$$p(\bar{P}_{z,\text{dB}}) = \frac{1}{\sqrt{2\pi}\sigma_{\text{dB}}} e^{-\frac{(\bar{P}_{z,\text{dB}} - \mu_{\text{dB}})^2}{2\sigma_{\text{dB}}^2}}, \quad (4)$$

where $\mu_{\text{dB}} = K_{\text{dB}} - 10\gamma \log d$ and σ_{dB} is the standard deviation of $\bar{P}_{z,\text{dB}}$. Consider the distance-dependent path loss, $\mu = K/d^\gamma$, where d represents the distance between the transmitting and receiving robots and γ denotes the power fall-off rate. Then, it can be seen from Eq. 4 that $\mu_{\text{dB}} = 10 \log \mu = K_{\text{dB}} - 10\gamma \log d$ represents the average of the large-scale variations. Note that $\bar{P}_r = \mathbb{E}[P_r]$ and SNR will also have lognormal distributions.

1) *Justification of Lognormal Distribution for Large-Scale Fading:* While several empirical data confirmed lognormal distribution to be a good fit for characterizing large-scale fading, there is also a mathematical justification for this distribution. Consider the n^{th} path from the transmitter to the receiver (as in one of the terms of Eq. 2). Each obstacle on the way of this path attenuates the transmitted signal. Let $l_{n,j}$ represent the distance the n^{th} path travels inside the j^{th} obstacle on its way. Let $\beta_{n,j}$ denote the decay rate of the wireless signal in the j^{th} obstacle. Then, we have

$$\alpha_{n,j,\text{obs}} = e^{-\beta_{n,j} l_{n,j}}, \quad (5)$$

where $\alpha_{n,j,\text{obs}}$ represents the attenuation caused by the j^{th} obstacle on the n^{th} path. This results in the following attenuation on the n^{th} path by all the obstacles:

$$\alpha_{n,\text{obs}} = e^{-\sum_j \beta_{n,j} l_{n,j}}. \quad (6)$$

By evoking the Central Limit Theorem, \log of $\alpha_{n,\text{obs}}$ will have a normal distribution, resulting in a lognormal distribution for large-scale fading.

Fig. 5 shows the pdf and cdf of large-scale fading for all the collected data in the basement of ECE building, as shown in Fig. 2, and for the transmitter at location#1. In order to access the large-scale variations, the gathered data of each route (such as the small-scale variations shown in Fig. 3) is averaged locally over small-scale fading. It should be noted that the large-scale variation is still non-stationary as its average changes with distance. The distance-dependent path loss component for each route can be easily estimated by finding the best linear fit that relates the \log of the received power of the collected data to $\log d$ (see Fig. 3 for an example). We then remove the distance-dependent average from large-scale variations before characterizing the distribution of the collected data. As a result, the distribution of the gathered data should match a zero-mean log-normal distribution. It can be seen, from Fig. 5, that the distribution of the \log of the large-scale variations (after removing the distance-dependent average) matches a zero-mean normal distribution very well. The standard deviation for this match is $\sigma_{\text{dB}} = 2.8$.

C. Distance-dependent Path Loss

It can be seen from Eq. 4 that the distance-dependent path loss, characterized as $K_{\text{dB}} - 10\gamma \log d$, is the average of the large-scale variations. This completes the relationship between the three underlying dynamics: small-scale fading, large-scale fading and path loss. As mentioned earlier, the distance-dependent path loss component can be found by finding the best linear fit that relates the \log of the received signal power to the $\log d$. For instance, for the data of Fig. 3, path loss component can be characterized as $-12.89 - 33 \log d$. It should be noted that the parameters of path loss curve, such as exponent γ , vary from route to route.

In current robotics and control literature, it is common to use disc models to model wireless channels. It is noteworthy that this over-simplified model only considers path loss. It furthermore assumes the same parameters for the path loss

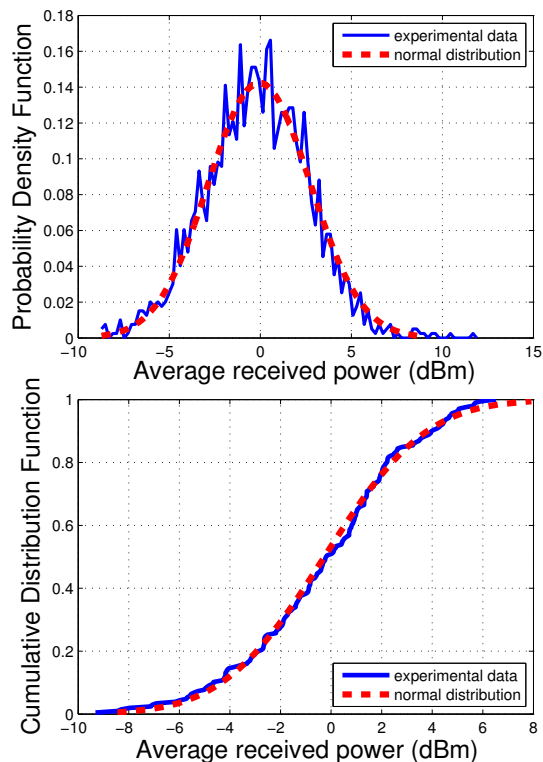


Fig. 5. (top) pdf and (bottom) cdf of the log of large-scale fading (after removing the distance-dependent path loss) for all the data gathered in the basement of ECE Bldg., and its normal distribution match.

of all routes in the environment. Therefore it is only a very crude representation after considerable averaging is done.

III. MODELING AND SIMULATION OF WIRELESS CHANNELS FOR NETWORKED ROBOTICS AND CONTROL

In this section, we briefly discuss different possibilities for modeling of wireless channels for the purpose of mathematical analysis or simulation in robotic networks. In general, what we know about the environment, in terms of locations and properties of objects, can play a key role in characterizing wireless channels.

A. Probabilistic Characterization

The probabilistic framework of the previous section is a powerful tool for both mathematical analysis involving wireless channels and developing simulation environments. Such probabilistic approaches have been extensively used in wireless systems literature since they generate channels that have similar behavior to real wireless channels. In particular, they are useful when little knowledge is available on the geometry and/or dielectric properties of the environment.

In order to generate a realistic wireless environment for both theoretical analysis as well as simulation environments, channel can be modeled as a non-stationary random process (small-scale fading) with a Rayleigh, Rician or Nakagami distribution. Then the average of the power of this process will have a lognormal distribution with a mean that follows the distance-dependent path loss. The parameters of the three dynamics can be varied to meet the level of fading that the

specific scenario requires. For a theoretical framework, this allows for a probabilistic analysis of the overall cooperative robotic performance.

Example 1: Consider the case where the goal of a robotic network is cooperative target tracking in a given area and in a limited time. The overall MSE of target trajectory estimation will then be a function of all link qualities. If the exact spatial map of the channel between any two nodes is not available (which is typically the case), then probabilistic analysis should be performed. In the area of interest, channels can be modeled probabilistically, based on the framework of the previous section. The final MSE becomes a random variable through its dependency on the channels. Then one can characterize the average of MSE (averaged over channel variables) or the probability distribution of it.

Example 2: In packet-dropping receivers, those packets with quality below a certain level are dropped. This translates to channel SNR being below a given threshold (SNR_{th}). Then the probability that a wireless link exists, between two nodes, can be easily calculated using the distributions of the previous section. For instance, for a Rayleigh-distributed small-scale fading, the probability that the link quality is above a certain threshold can be characterized as follows:

$$\text{Prob}(\text{link exists}) = \text{Prob}(\text{SNR} > \text{SNR}_{\text{th}}) = e^{-\text{SNR}_{\text{th}}/\overline{\text{SNR}}},$$

where $\overline{\text{SNR}}$ represents the average of SNR over small-scale fading. However, we know from the analysis of the previous section that SNR is non-stationary unless the considered distances are small enough. As a result, $\overline{\text{SNR}}$ will be a random variable itself:

$$\log \overline{\text{SNR}} \sim \text{normal R.V. with mean following path loss.}$$

This means that the probability that a link exists should be modeled as a random process whose distribution can be derived using the distribution of large-scale fading and distance-dependent path loss.

1) *Which Scale to Use?:* As was seen in the previous section, there are three underlying scales associated with a wireless channel. Depending on the scenario, all or some of these scales should be considered. For instance, if the area of interest is small enough, only considering stationary small-scale variations could be enough. For most robotic applications, however, the distances travelled could be large enough that large-scale variations and path loss should also be considered. If the distance between consecutive channel usages is large enough, large-scale variations and path loss could also become dominant factors.

2) *Channel Spatial Correlation:* Thus far we discussed characterizing the distribution of a wireless channel at a single position (or equivalently at a time instant). What is left is a characterization of channel spatial correlation, i.e. how fast the small-scale and large-scale fading components are changing spatially. Depending on the speed of the robots and how often they are communicating, channel could be assumed spatially uncorrelated. In general though, a wireless channel is spatially correlated. Spatial correlation of small-scale fading depends on the speed of the robots, frequency

of operation and antenna beamwidth/gain, among several other factors. The least correlation is typically observed when there exists a rich scatterer/reflector environment that results in a uniform angle of arrival of the paths. In such cases, the Fourier transform of the auto-correlation function of small-scale fading will have a form that is referred to as Jakes spectrum [1] and channel uncorrelates on the order of 0.4 times the wavelength (5 cm for 2.4 GHz WLAN transmission). If this is not the case, spatial correlation function of small-scale fading can be mathematically derived for a general case [1]. Double mobility (the case where both transmitting and receiving nodes are moving) has an interesting effect on small-scale fading as it is shown to increase its spatial correlation [4]. For large-scale fading, there is less mathematical characterization of spatial correlation. Gudmundson [5] characterizes an exponentially-decaying spatial correlation function for large-scale fading, based on outdoor empirical data, which is widely used.

B. Case of Known Environment

If all the information about object positions, geometry and dielectric properties is available, ray tracing methods could be used to find a spatial map of the received signal strength in the area of interest. A ray tracer [6] follows all or some of the reflected, diffracted or scattered multipaths in the environment. There are several developed software, such as Wireless InSite [7] and Motorola's Wireless LAN Planner and Site Scanner, that are aimed at generating a map of the received signal strength based on ray tracing. While it is possible to use such software for evaluating the performance of a robotic network in a certain environment, assessing the exact coefficients associated with the dielectric properties of the objects could be challenging. Furthermore, unlike probabilistic characterizations of the previous section, ray tracing approaches are not suitable for mathematical analysis since they simply generate a received signal map for a specific environment.

C. Case of Partially Known Environment

While it may not be possible to know all the specifications of the environment of interest, partial knowledge on the objects may be available. In robotic applications, the positions and geometry of some of the objects are learned for navigation purposes. Such knowledge can be used to generate an approximated map of the received signal strength. For instance, the received signal power in dB, $P_{r,\text{dB}}$, at position \vec{x} , can be approximated as follows by following the LOS path and considering only large-scale fading and path loss:

$$P_{r,\text{dB}}(\vec{x}) \approx \underbrace{P_{T,\text{dB}}}_{\text{TX power}} + \underbrace{K_{\text{dB}} - 10\gamma \log d}_{\text{path loss } (\leq 0)} - \underbrace{\zeta \sum_j \hat{\beta}_{\text{los},j} l_{\text{los},j}}_{\text{large-scale fading}} \quad (7)$$

where $\zeta = 10/\ln(10)$, path loss parameters are as defined earlier and $\hat{\beta}_{\text{los},j}$ and $l_{\text{los},j}$ denote the approximated decay rate of the LOS path and its travelled distance in the j^{th} obstacle on its path respectively. Other terms can be added to account for reflections, scattering or diffraction. However,

predicting the exact received signal strength map, based on partial knowledge, is considerably challenging and can amount to non-negligible errors. For simulation purposes, one can also combine partial environment-specific knowledge with probabilistic components in order to generate a more realistic channel. For instance, a small-scale fading variable can be added to the received power generated from Eq. 7. Fig. 6 shows simulated binary maps of the received signal power where black areas indicate regions with the received signal strength below an acceptable threshold while white areas denote otherwise. The left figure shows an example of a channel generated based on knowing the positions of the obstacles and considering only large-scale fading and path loss, as indicated by Eq. 7, and for the transmitter location as indicated. The right figure shows the same map after adding a Rician-distributed small-scale fading to it, which shows a more realistic case.



Fig. 6. Examples of a binary channel (white areas indicate that channel quality is above a threshold) – (left) channel generated based on knowing the positions of the obstacles and considering only large-scale fading and path loss and (right) the same channel after adding Rician-distributed fading.

IV. CONCLUSIONS

The goal of this paper was to provide a reference for researchers in robotics and control that are interested in realistic characterization of wireless links. By utilizing the knowledge available in wireless communication literature, we provided a comprehensive overview of the key characteristics of wireless channels: small-scale fading, large-scale fading and path loss, for networked robotic and control operations. We furthermore confirmed these mathematical models with channel measurements made in our building. Finally, we discussed channel characterization based on the knowledge available on the environment.

V. ACKNOWLEDGMENT

The authors would like to thank Dr. Fierro for lending them the robots for the experimental setup.

REFERENCES

- [1] W. C. Jakes, *Microwave Mobile Communications*. New York: Wiley-IEEE Press, 1994.
- [2] T. S. Rappaport, *Wireless Communications: Principles and Practice*. Upper Saddle River, NJ, USA: Prentice-Hall, 2002.
- [3] A. Goldsmith, *Wireless Communications*. New York: Cambridge University Press, 2005.
- [4] R. Wang and D. Cox, "Double mobility mitigates fading in ad hoc wireless networks," in *IEEE International Symposium on Antennas and Propagation*, vol. 2, pp. 306–309, 2002.
- [5] M. Gudmundson, "Correlation model for shadow fading in mobile radio systems," *Electronics Letters*, vol. 27, pp. 2145–2146, Nov. 1991.
- [6] C. F. Yang, B. C. Wu, and C. J. Ko, "A ray-tracing method for modeling indoor wave propagation and penetration," *IEEE Transactions on Antennas and Propagation*, vol. 46, pp. 907–919, Jun 1998.
- [7] <http://www.remcom.com/wireless-insite/>.